Wind and Structures, *Vol. 26, No. 6 (2018) 369-382*
DOI: https://doi.org/10.12989/was.2018.26.6.369

A comparison of the forces on dome and prism for straight and tornadic wind using CFD model

Majdi A.A. Yousef[*1], Panneer R. Selvam[1a] and Jai Prakash[2b]

[1]Department of Civil Engineering, University of Arkansas, 4190 Bell Engineering, Fayetteville, AR, 72701, USA
[2]Department of Mathematics, University of Botswana, Private Bag UB 0022 Gaborone, Botswana, Southern Africa

(Received December 4, 2016, Revised January 27, 2018, Accepted March 6, 2018)

Abstract. Tornadoes are vertical swirling air formed because of the existence of layers of air with contrasting features of temperature, wind flow, moisture, and density. Tornadoes induce completely different wind forces than a straight-line (SL) wind. A suitably designed building for an SL wind may fail when exposed to a tornado-wind of the same wind speed. It is necessary to design buildings that are more resistant to tornadoes. In tornado-damaged areas, dome buildings seem to have less damage. As a dome structure is naturally wind resistant, domes have been used in back yards, as single family homes, as in-law quarters, man caves, game rooms, storm shelters, etc. However, little attention has been paid to the tornadic wind interactions with dome buildings. In this work, the tornado forces on a dome are computed using Computational Fluid Dynamics (CFD) for tornadic and SL wind. Then, the interaction of a tornado with a dome and a prism building are compared and analyzed. This work describes the results of the tornado wind effect on dome and prism buildings. The conclusions drawn from this study are illustrated in visualizations. The tornado force coefficients on a dome building are larger than SL wind forces, about 120% more in *x*- and *y*-directions and 280% more in *z*-direction. The tornado maximum pressure coefficients are also higher than SL wind by 150%. The tornado force coefficients on the prism are larger than the forces on the dome, about 100% more in *x*- and *y*-directions, and about 180% more in *z*-direction. The tornado maximum pressure coefficients on prism also are greater those on dome by 150% more. Hence, a dome building has less tornadic load than a prism because of its aerodynamic shape.

Keywords: tornado wind; CFD simulation; force and pressure coefficients; dome and prism building

1. Introduction

In the last ten years alone in the United States, there were about 1,200 tornadoes which caused about 1,150 injuries, 100-105 deaths and at least 2.3 billion dollars in economic damage, as reported by the American National Weather Service (NWS, 2017). In order to reduce the human and property damages, it is necessary to design structures that are more resistant to tornadoes. The understanding of the tornado interaction with a structure is necessary to reduce those human and property damages. Although the investigation of tornado-structure interaction has increased, the behavior of tornado-structure interaction has not been sufficiently explored, which justifies the necessity of the research in this study. The first requirement for accomplishing this goal is a better understanding of tornado-structure interaction and tornado-induced loads on buildings. The development in tornado wind modeling can induce a better calculation of tornado maximum forces. Then, the result can be applied to improve the design standards. Thus, researchers have started studying the tornadic wind fields and wind effects on structures in laboratory tornado simulators or using CFD model.

Early Wen (1975) started the research on tornado-structure interaction. He defined the effects of inertia and drag forces. Wen (1975) utilized semi-empirical equations based on the principles of fluid dynamics. McDonald and Selvam (1985) questioned the validity of Wen's procedure using computer simulation and established potential flow simulation around 2D sections using the mathematical model, Rankine Combined Vortex (RCV) model. They recommended modifications to the application of the inertia forces from Wen's method. The time dependent boundary conditions are reported in detail in Selvam (1985). Then, Selvam (1993) applied the RCV model to study flow around the Texas Tech building using the k-ε model. In this model, the boundary layer effect is included by varying the wind field with a logarithmic profile. There were some difficulties in applying proper boundary conditions using the k-ε model. To alleviate this problem, Selvam and Millett (2003 and 2005) employed large eddy simulation as a turbulence model and obtained reasonable results for flow around a cube. They concluded that the translating tornado produced about 100 % force on the roof and about 45% more on the walls compared to wind loads.

Alrasheedi and Selvam (2011) investigated the tornado impact on buildings with different plan area sizes using the CFD model, presented by Selvam and Millet (2003). They

*Corresponding author, Ph.D.
E-mail: myousef@uark.edu
[a] Professor
E-mail: rps@uark.edu
[b] Professor
E-mail: prakashj@mopipi.ub.bw

http://www.techno-press.com/journals/was&subpage=7 ISSN: 1226-6116 (Print), 1598-6225 (Online)

reported that tornado force coefficients on buildings, which have a much wider plan area than the tornado radius, are similar to the straight boundary layer wind force coefficients. Selvam and Gorecki (2012) studied an influence of the different ratios for tornado size to circular cylinder size on the tornado forces. They found that tornado forces depend on the size of the building. When the building size decreases, comparing to the tornado size, the forces increase. The study was conducted up to ratio of a 30:1. They concluded that the tornado forces tend to be constant when tornado to cylinder ratio is more than 18:1. Although the aforementioned studies are about vortex-structure interaction in 2D, they reveal the effect of structure size on tornado forces. Strasser and Selvam (2015) studied the influence of relative vortex-to-circular cylinder size on structural loading. They used 2D simulation to study the force coefficients around circular cylinder for vortices having radii of 1·D to 100·D. They concluded that the vortex no longer influences maximum force coefficients on cylinder when $r_{max} \geq 20D$; however, force coefficients do not reach their asymptotic value until $r_{max} \geq 50D$; where r_{max} and D are critical radius for the vortex and diameter of the cylinder, respectively. Selvam and Gorecki (2015) and Selvam and Ahmad (2016) also used the modified version of a CFD model, reported by Selvam and Millet (2003), to study the interaction between a tornado and a longitudinal hill. They found that the hill creates a sheltering region on the hill leeward side.

Recently, Iowa State University (ISU), Texas Tech University and Western University (WU) developed their tornado simulators. Haan *et al*. (2010) and Hu (2011) used the ISU simulator to investigate the wind flow around a one-story, gable-roofed building in tornado-like winds as well as the wind effects on this structure. They reported that the tornado-induced lateral forces were about 50% larger than those by ASCE 7-05 and the tornado-induced vertical force were two or three times as large as those by the provision. Sengupta *et al.* (2008) investigated the influence of the translating speed on wind effects through a cubic building using the tornado simulator at ISU. They reported that a lower translating speed induces greater wind loading on the structure. Yang *et al.* (2010) utilized a laboratory tornado simulator to evaluate wind fields around a gable-roofed building, caused by a stationary tornado and a SL wind. They showed that both of the flows, around structures, are different. Rajasekharan *et al.* (2013) applied the tornado simulator (Ward type) at Tokyo Polytechnic University (TPU) to gain a better understanding of the effect of building location with respect to the tornado center. Sabareesh *et al.* (2013) utilized TPU tornado simulator to investigate the effect of ground surface roughness on the internal pressures developed inside a building model. Ishihara *et al.* (2011) investigated how the swirl ratio affects the shapes of the generated tornado with large eddy simulation (LES) to model turbulence.

Zhao *et al.* (2016) studied the flow and pressure around a dome due to SL and tornado wind by moving the dome, but they did not have proper grid resolution. They moved the dome by dynamic mesh method, and at each time step, they deformed the mesh and generated or eliminated elements. In this simulation, the building can be moved only in the allowed region of the vortex chamber. They concluded absolute maximum pressure induced by tornadic winds is found to be 240% more than those induced by SL winds. The authors also reported that the wind vertical force coefficients obtained in the tornadic wind field is 270% more than those in the SL wind field. However, the lateral force coefficient (in the x-direction) induced by the tornadic winds is 600% more than those induced by the SL winds. Most of the recent research of the effects of tornado force on buildings has been done on non-dome buildings. A preliminary study of investigating the interaction of tornado wind with different structures such as dome and prism, in order to reduce the human and property damages (Yousef and Selvam 2016). This study is necessary to design structures that are more resistant to tornadoes. They compared the force and pressure coefficients around a dome and prism building under the influence of SL and tornado wind by moving the tornado. They concluded that tornadoes induce completely different wind forces on both dome and prism buildings than a straight-line (SL) wind. They concluded the absolute maximum pressure induced by tornadic winds is found to be 60% more than that induced by SL winds. They concluded that the translating tornado produced about 120% force on the roof and about 65% more on the walls compared to wind loads. In the current study, a further refined grid is used for detailed investigation.

1.1 Field observation of tornado interacting with prism and dome type of structures

In the tornado-damaged areas, dome buildings seem to have less damage. In one instance, 1,700 homes were destroyed by EF4 or EF5 tornado in Moore, Oklahoma (2013). In the middle of all this destruction only one simple concrete dome structure survived as illustrated in Fig. 1 (Monolithic 2013). In another instance, a wood dome house survived after it was hit by the EF5 tornado in West Jefferson County as shown in Fig. 2 (New Age Dome Construction 2017). From these observations, one can say that the dome shape may have reduced the forces. As a dome structure is naturally wind resistant, domes have been used in back yards, as single family homes, as in-law quarters, man caves, game rooms, storm shelters, etc. (Monolithic 2013). However, the tornado forces and pressure on dome structure and other structures such as cube, prism and gable roof have never been compared.

Fig. 1 Dome survived in Moore, Ok (Monolithic 2013)

Fig. 2 Dome survived with partial failure (New Age Dome Construction , 2016)

1.2 Objective

Despite the above research, the wind effects of tornadoes on dome buildings have not been sufficiently explored, which justifies the necessity of the research in this study. Moreover, the forces and pressure on the dome and prism have not been compared. Thus, the interaction of a tornado wind with a dome and a prism building need to be compared and analyzed. Then, the outcome can be implemented for improving building design standards that may reduce tornadoes fatalities and property damage. Thus, the modified version of Selvam and Millett (2003, 2005) model is applied to reveal the physics of the RCV model interaction with buildings (e.g., dome and prism). The primary objective of the work is to identify the pressure and force differences between dome and prism. The investigation is focused on the visualization of vortex shape and strength during the integration. Then, the force and pressure coefficients on dome and prism due to straight-line (SL) and tornadic wind are compared.

2. Computer modeling

Since tornado-structure interaction is a complex phenomenon, CFD model has been utilized to clarify and understand this phenomenon. Therefore, the Computational Mechanics Laboratory of the University of Arkansas has been involved in the computer modeling of tornado forces on buildings for more than 30 years. In these research findings, the building is assumed to be rigid.

2.1 Fluid-structure interaction modeling

The flow around the structure is computed by solving the Navier-Stokes (NS) equations. The turbulence is modeled using Large Eddy Simulation (LES). The flow equations are approximated by either Finite Element Method (FEM) or Finite Difference Method (FDM). The FDM code has been used previously by Selvam and Millett (2003 and 2005) to study flow over cubic building. This is based on orthogonal grid system, and it is computationally very efficient. They have examined how to apply finite number of different procedures on rectangular grids. The same code is used to compute the forces around the rectangular prism (Gorecki and Selvam 2015, Alrasheedi and Selvam 2011). The FDM code based on orthogonal grid system was developed to study flow around a dome, but it had more error in transporting the tornado-like vortex. For dome problems, the scheme needs to have greater geometrical flexibility. To consider a curved boundary, a better solution is to use a body-fitted grid that follows the domain geometry. Hence, the FEM code based on body-fitted grid was developed to study flow around a dome. Ahmad and Selvam (2015) used this numerical model to study the tornado-terrain interaction. They validated this numerical model by comparing the results with experiments. The detail of the equations and methods are documented by Ahmad and Selvam (2015). The superiority of FEM to FDM in transporting vortices is reported in Selvam (1998). The FEM code takes more computer time and hence parallel computing is utilized by Ahmad and Selvam (2015). They used single- and multi-processors to find the optimum number of processors which provide the minimum run-time. They concluded that 24 processors provide the minimum run-time which is 72 hours for problems of 7.569 million points.

2.2 Navier-Stokes equations and convergence criterion

The NS equations for the incompressible flow used to simulate the vortex flow:

Continuity Equation

$$U_{i,i} = 0.0 \tag{1}$$

Momentum Equation

$$U_{i,t} + U_j U_{i,j} = -(\frac{p}{\rho} + \frac{2k}{3})_{,i} + \left[(\nu + \nu_t)(U_{i,j} + U_{j,i})\right]_{,j} \tag{2}$$

Where

$$\bar{S}_{ij} = U_{i,j} + U_{j,i} \tag{3}$$

$$\nu_t = (C_S h)^2 \left[2(S_{i,j})^2\right]^{\frac{1}{2}} \tag{4}$$

$$h = (h_1 h_2 h_3)^{\frac{1}{3}} \tag{5}$$

$$k = \frac{\nu_t^{\,2}}{(C_K h)^2} \tag{6}$$

Where: *Ui*, is the mean velocity, *p* is the mean pressure, *Vt* is the turbulent eddy viscosity, *Vi* is the velocity of grid, *k* is the turbulent kinetic energy, and ρ is the fluid density. The variables *h1*, *h2* and *h3* control volume spacing in the *x*-, *y*-, and *z*- directions, respectively. The area or volume of the element is used for the computation of *h*. A comma represents differentiation, t represents time, and i=1, 2 and 3 refers to variables in the x-, y- and z- directions. The Cs and Ck empirical constants are taken to be, respectively, 0.1 and 0.094, as proposed by Murakami and Mochida (1995). Selvam (1997) found an excellent agreement between flow field over a structure and the LES simulation for the Cs and Ck values proposed by Murakami and Mochida in 1995. In this work, a procedure is used to solve the unsteady NS equations in which the momentum equation is used to solve velocities; then, the new velocities are used to solve the pressure. The final form of pressure equation is

$$\Delta p = \frac{\left(\frac{\partial U}{\partial x}+\frac{\partial V}{\partial y}+\frac{\partial W}{\partial z}\right)}{\Delta t} - \left[\frac{\partial\left(U\frac{\partial U}{\partial x}+V\frac{\partial U}{\partial y}+W\frac{\partial U}{\partial z}\right)}{\partial x} + \frac{\partial\left(U\frac{\partial V}{\partial x}+V\frac{\partial V}{\partial y}+W\frac{\partial V}{\partial z}\right)}{\partial z} + \frac{\partial\left(U\frac{\partial W}{\partial x}+V\frac{\partial W}{\partial y}+W\frac{\partial W}{\partial z}\right)}{\partial z} \right] \tag{7}$$

Where: U, V, and W are the velocities in x, y and z directions, P and Δt are the pressure over density and the time step, respectively. Here U, V and W are the velocities in the x-, y- and z- direction, P is the pressure over density and Δt is the time step. The above sequential procedure is a general version of the one used by de Sampio *et al.* (1993) using least square FEM. The procedure is also similar to Selvam and Paterson (1993) and Tamura (1995 , 1999) using FDM.

The equations are solved in time using a semi-implicit method, as suggested by Selvam (1997). For an approximation of continuity and momentum equations, the four-step development system is utilized:

(1) Solve for Ui from Eq. (2). The diffusion and convection terms are considered implicitly. The pressure is considered on the right-hand side of the equation. For simplicity, here p/ρ is considered as p.

(2) Find new velocities as $U'i = Ui + \Delta t{\cdot}p,i$ where Ui' is not specified.

(3) Solve for pressure from $p,ii = U'i,i/\Delta t$.

(4) Correct the velocities for incompressibility: $Ui = U'i - \Delta t{\cdot}p,i$

Step 2 eliminates the checkerboard pressure field when using equal order interpolation for velocity and pressure in the case of either a finite element method or finite difference method. The time step is calculated according to the Courant-Frederick-Lewis (CFL) number. The CFL number is kept to less than one; this gives time step around 0.01 units for most of the computation. The velocity equations are solved by line iterations in x-, y- and z- directions. In each time step, the velocities are calculated successively in the implicit method. The iterations are repeated to the convergence value. That value is defined to be IM × JM × KM × 10^{-5}, where IM, JM and KM are number of grid points in the x-, y- and z- directions.

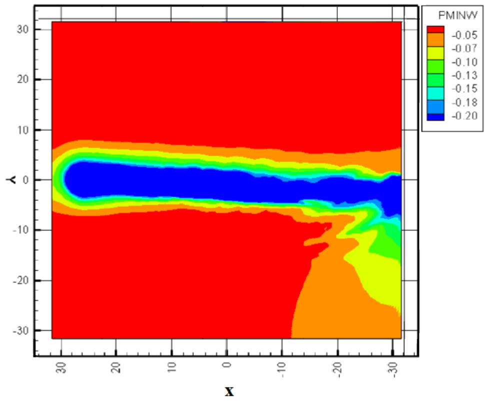

Fig. 3 Minimum pressure on the domain ground

The computation of the vortex-prism interaction takes about 20 days to conduct a single simulation for about 6.2 million grid points. The computation of the vortex-dome interaction takes about 5 days using 24 processors for approximately 7.5 million grid points. The output file is about 1.4 GB per time step. More details about parallel computing can be found in Ahmad and Selvam (2015).

2.3 Vortex transportation on a flat terrain

The vortex transports along the x-axis, and monitor the minimum pressure on the numerical domain ground to understand the overall pressure distribution along the surface of the building. The vortex is transported completely along the x-axis of the domain, and the flat terrain (no building effects) is considered for this resolution. From Fig. 3, one can see that the tornado path is almost a straight line. It was noticed that there is reduction in the width of the minimum pressure about 25%. This reduction happened because of the loss in the vortex strength due to turbulent dissipations. However, that reduction is acceptable since only the path deviation is monitored.

2.4 Vortex flow modeling, boundary conditions and grid size

The geometries of the problems for this study are illustrated in Figs. 4(a) and 4(b). The counterclockwise rotating vortex travels along the x-axis with a constant velocity V_t. The vortex flow and free stream of a constant velocity is smoothly introduced into the computational domain. The two cases of vortex-building interaction are analyzed, namely vortex-dome interaction and vortex-prism interaction. The free stream velocity magnitude and its direction are equal to the translational velocity of the vortex. To have one to one correspondence with respect to height and the projected area in the z-direction, the width of the dome and prism are assumed to be 20.0 m and 17.72 m, respectively. The height of the dome and prism are assumed to be 10.0 m. Instead of taking the same projected area of the dome and prism, in future study, the same volume of the dome and prism also will be taken. In the current study, the focus is on same projected area in z-direction and the same height. The numerical computations are conducted based on the non-dimensional value. The height of the dome and prism (H) is considered to be the reference value. Then width of the dome and the prism (D) comes to be 2.0H and 1.77H non-dimensional (ND) units. The translational velocity is considered to be the reference velocity. The Reynolds number based on the height of the building is $Re = 1.2 \times 10^6$. The vortex based Reynolds number is $Rev = \Gamma/\nu$, which is 5.7×10^6, where Γ is the RCV circulation.

2.4.1 Vortex flow modeling

To simulate tornado travel over a building, the three-dimensional CFD model is used. The tornado wind field model is studied by applying Rankine Combined Vortex (RCV) model which is the simplest computer model that can satisfy the Navier-Stokes (NS) equations as reported in Lewellen (1976). According to Doppler radar data of real tornadoes, the horizontal and vertical wind velocity distribution changes amongst tornado outbreaks. (Wurman *et al.* 2007, Kosiba *et al*. 2014). In addition, a tornado's structure constantly changes during travel. This is performed in various tornado mathematical models. In the current study, the assumption of the tornado vortex model is controlled by the numerical modeling requirements. Amongst the retrieved tornado velocity models, the RCV model satisfies the NS equations as well as shows a tornado velocity distribution. The RCV model only assigns horizontal velocities, whereas there is no control on the vertical velocities in the simulation. As the vortex is transported downstream, vertical velocities are developed in the simulation by self-induced conditions as reported in Filipone and Afgan (2008) and Gorecki and Selvam (2014).

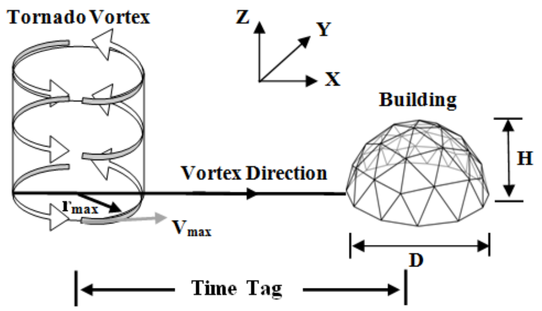

(a) Vortex- dome interaction

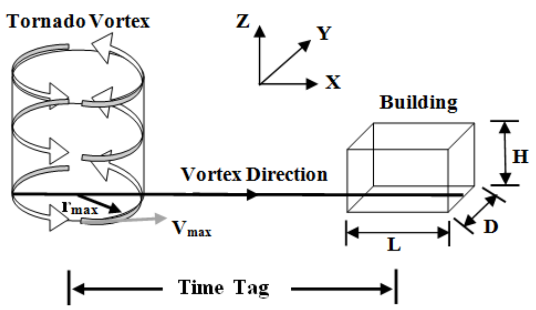

(b) Vortex – prism interaction

Fig. 4 Problem geometry

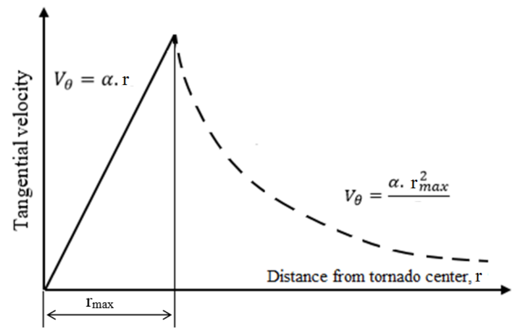

Fig. 5 The Rankine Combined Vortex of tornado velocity

The RCV model consists of two different flow fields which are the forced vortex region, or the vortex core ($r \le r_{max}$), in the free vortex region ($r > r_{max}$). For $r \le r_{max}$, the tangential velocity of the tornado V_θ, increases linearly up to vortex radius r_{max}, where r is the distance from the center of the tornado and α is a vortex core strength constant as shown in Fig. 5. For $r > r_{max}$, the tangential velocity is hyperbolically decreasing. In this model, a translational velocity V_t, and the building is overlapped onto the RCV model wind field in addition to the vertical logarithmic difference to calculate the boundary layer as stated by Selvam (1993). Inside the RCV model, the flow speeds are equal to 0.0. The RCV model satisfies the conservation equations, so that the vortex overlap does not produce any abnormality. The tornado vortex is held only in the forced vortex region, or the vortex core. Outside the vortex core in the free vortex region, the vorticity is equal to 0.0.

2.4.2 Boundary conditions

The simulated flow is a consequence of time-dependent boundary conditions utilized over the simulation time on the domain boundaries, as illustrated in Fig. 6. The building (e.g., dome and prism) is located at a reasonable distance from the boundary of the computational domain. The velocities are considered to be zero on the surface of the rectangular prism and hemispherical dome (no-slip condition). The logarithmic law is used to model the boundary layer (Eq. (10)). The boundary layer of building is resolved by the grid. Making an allowance for the starting point, both the *x*- and *y*- axis are located at the center of the building, and *z*-axis is located on the ground. When the center of the tornado overlaps with center of the building, the time *t* is zero. The velocity components in the *x*- and *y*-directions are expressed as follows

$$\left.\begin{aligned} U(_{x,y,z,t}) &= \left[(V_t - y)\times\alpha\right]z_f && for\ \ r \le r_{\max} \\ U(_{x,y,z,t}) &= \left[(V_t - y)\times\frac{\alpha r^2{}_{\max}}{r^2}\right]z_{fl} && for\ \ r > r_{\max} \end{aligned}\right\} \tag{8}$$

$$\left.\begin{aligned} V(_{x,y,z,t}) &= \left[(x - V_t t)\times\alpha\right]z_f && for\ \ r \le r_{\max} \\ V(_{x,y,z,t}) &= \left[(x - V_t t)\times\frac{\alpha r^2{}_{\max}}{r^2}\right]z_f && for\ \ r > r_{\max} \end{aligned}\right\} \tag{9}$$

Because the RCV model does not include any condition for the vertical velocity component, w = 0. In Eqs. (8) and (9), Z_f is applied to form the domain surface boundary layer based on the logarithmic law

$$Z_f = \frac{u*}{k}\ln\left(\frac{z+z_0}{z_0}\right) \tag{10}$$

Where z is the height from the ground, $u*$ is the frictional velocity which is computed from the recognized velocities at known height, z_0, the surface roughness length, is considered to be 0.00375. A schematic of this equation is offered in Fig. 7. κ= 0.4, on boundary faces the normal derivative of pressure is assumed to be zero, p = 0. The calculation is made on the orthogonal grid and the RCV model is transported to the Cartesian coordinates as

$$r^2 = (x - V_t t)^2 + y^2 \tag{11}$$

More details about the derivation can be found in Selvam (1995). The NS equations are used for solving the interior velocities and pressures at each time step. The computational domain is a rectangular block with non-dimensions value 60.0H x 60.0H x 45.0H units. The numerical computations are managed based on the dimensionless values to simplify the computation. The dimensionless length, velocity and time (respectively: L^*, U^*, t^*) are calculated as follows

$$L^* = L / L_{ref} \tag{12}$$

$$U^* = U / V \tag{13}$$

$$t^* = t.V / L_{ref} \tag{14}$$

Where: L, U and t are length, velocity and time; $Lref$ – referenced length equal to the height of the hill; V – referenced velocity, equal to the translational velocity. The tornado parameters are stated in Table 1. The ratio of tangential velocity (V_Θ) to translational velocity (V_t) of real tornado is (3-4) as detected from National Weather Service Weather Forecast Office (2011). In the current study, a translation velocity is chosen 1.0 unit (10 m/s) in order to apply the V_Θ/Vt ratio of real tornado. Kosiba *et al.* (2014) reported that the tangential velocity, found on the vortex core radius, is equal to 3.0 units (30 m/s). Therefore, the ratio of tangential velocity (30 m/s) to translation velocity (10 m/s) is 3 which is in agreement with ratio V_Θ/V_t of real tornado. The maximum horizontal flow velocity is 4.0 units (40 m/s) which is a sum of the translational velocity and the tangential velocity. The total simulation time is 60 units. The simulation starts at t = −30 units and ends at t = 30 units. To avoid the use of negative time values, the time axis was moved forward by 30 units.

Table 1 Tornado Parameters

Units	α	r_{max}	V_t	V_θ	V_{max}
Non-dimensional	1.0	3.0	1.0	3.0	4.0
S.I. units	1.0 1/s	30 m	10 m/s	30 m/s	40 m/s

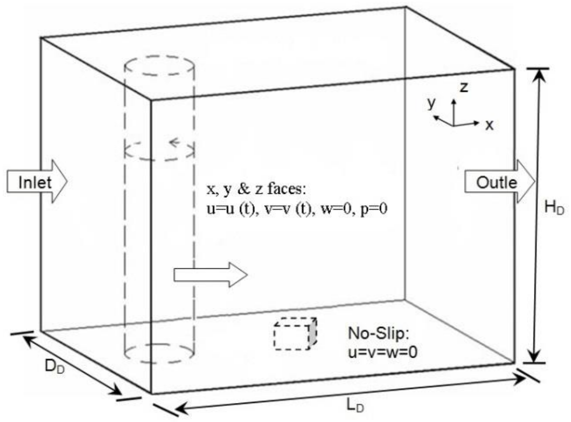

Fig. 6 Boundary conditions

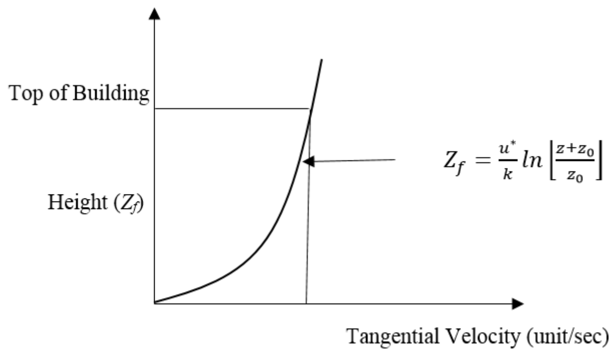

Fig. 7 The tangential velocity with decreasing height

2.4.3 The grid size on the simulated vortex

In the CFD vortex-structure simulation, the parameters of the simulated vortex and those applied in the boundary conditions are often assumed to be similar (Selvam and Millet 2005, Liu and Marshall 2004). The force and pressure coefficients are calculated using the maximum velocity (V_{max}) at the height of the building. The velocity value of provided tornado is computed based on its location. The velocity value where V_t and $V\theta$ are parallel and in the same direction (the stronger side of the tornado) is higher than the value where V_t and V_θ are in opposite direction (the weak side of the tornado). Therefore, The maximum velocity (V_{max} = V_t and V_θ). The correction was made. When extending the vortex into the vertical axis, attention needed to be given to how the velocities may vary with respect to height. In actual atmospheric vortices, the tangential velocity and the core radius of the tornado are reduced as the height in the z-direction approaches ground level due to the effect of the boundary layer (Fig. 7). In order to account for reduction in the velocity, an exponential growth function is applied to the tangential velocity calculations. Eq. (10) applied for this growth. The vortex structure and strength over the simulation are changed by the dissipative and the convective effects. Those effects are reliant on quality of the computational domain grid and dimensions. Unless a properly resolved grid is used, the dissipative and dispersive error in modeling the convection term will be high. The simulations presented in this section are similar to those conducted by Gorecki and Selvam (2014). They verified the influence of the domain and the mesh on the simulated vortex. They suggested that the fine grid spacing of 0.25H is applied only on the 6 × r_{max} wide lane on the vortex path and around the dome and prism. Outside the path the grid spacing is equal to 0.75H. That reduced the total number of grid points and the run-time of the simulation. The dome and prism boundary layer is resolved by fine grid refinement. The first grid spacing next or close to the dome and prism buildings is assumed to be 0.0055H as suggested by Selvam and Millet (2005). Where, H is a structure's height. The logarithmic law is concerned with the ground boundary layer but a refined grid is not required. The computational grids for the dome and prism models in xy-plane are illustrated in Figs. 8(a) and 8(b). The computer model presented in the current study is the same as the one used by Selvam and Millett (2005) and Gorecki and Selvam (2015). Therefore, the grid refinements suggested by authors are used in the current study in order to avoid repetition of research.

<u>*Nomenclature*</u>

The force coefficients are calculated using the following equations

$$Cx = F_x/(0.5\rho V^2 A) \tag{15}$$

$$Cy = F_y/(0.5\rho V^2 A) \tag{16}$$

$$Cz = F_z/(0.5\rho V^2 A) \tag{17}$$

$$Cp = \Delta p/(0.5\rho V^2) \tag{18}$$

Where the tornado force coefficients (*Cx*, *Cy*, and C_Z) were computed along the *x*-axis (horizontal direction parallel to the tornado's translation direction), *y*-axis (horizontal direction perpendicular to the tornado's translation direction), and *z*-axis (vertical) directions. The *x*- and *y*-coefficients are normalized with an area equal to the projected plan of the model in *x*- and *y*- directions, respectively. The *z*-coefficient was normalized with an area equal to the floor plan of the model. *Fx, Fy* and *Fz* are respective forces in *x*-, *y*-, and *z*-directions, ρ is the density of air, *V* is the reference velocity and ν is the kinematic viscosity of air, *Cp* is the mean pressure coefficient, *Δp* is the pressure difference, and *P* - *Pref* (*Pref* is equal to 0.0).

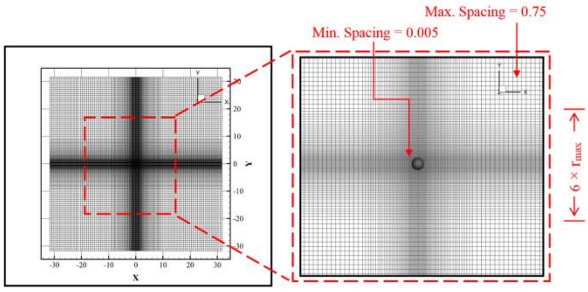

(a) Vortex– dome building interaction

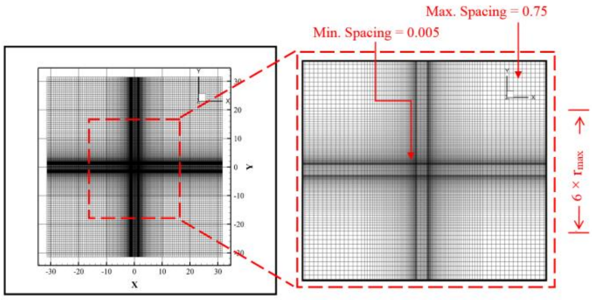

(a) Vortex-prism buildings interaction

Fig. 8 Computational grid in x-y plane

The reference velocity in the tornado wind field is the maximum velocity which is equal to $V_\theta+V_t$. By integrating the pressure in each direction on the surface, the forces are computed.

3. Results and discussion

3.1 Force and pressure coefficients due to SL wind

The computed force and pressure coefficients for SL wind is compared with the ASCE 7-10 to determine if the computer model values are relevant to ASCE 7-10.The three dimensional contours of the minimum and maximum pressures for the dome and the prism buildings are illustrated in Figs. 9(a)-9(d). The absolute maximum negative and positive pressures on the dome are - 0.8 and 0.5, respectively. The maximum effect of the negative pressure is seen close to the top of the dome, and the positive pressure is seen closer to the ground. The absolute maximum negative and positive pressures on the prism are – 2.0 and 0.5, respectively. The maximum effect of the negative pressure is seen on the roof and walls of the prism close to the sharp edge and corners, and the positive pressure is seen more on the walls of the prism building. The prism has higher maximum negative pressure than the dome, about 150% more. However, the maximum positive pressure on dome and prism are quite similar.

The force coefficients are calculated by integrating pressure all over the building (Figs. 10(a) and 10(b)). The maximum *Cx*, *Cy*, and *Cz*, values for the dome and prism are 0.32, 0.0, 0.25; and 0.84, 0.0, and 0.8 respectively.

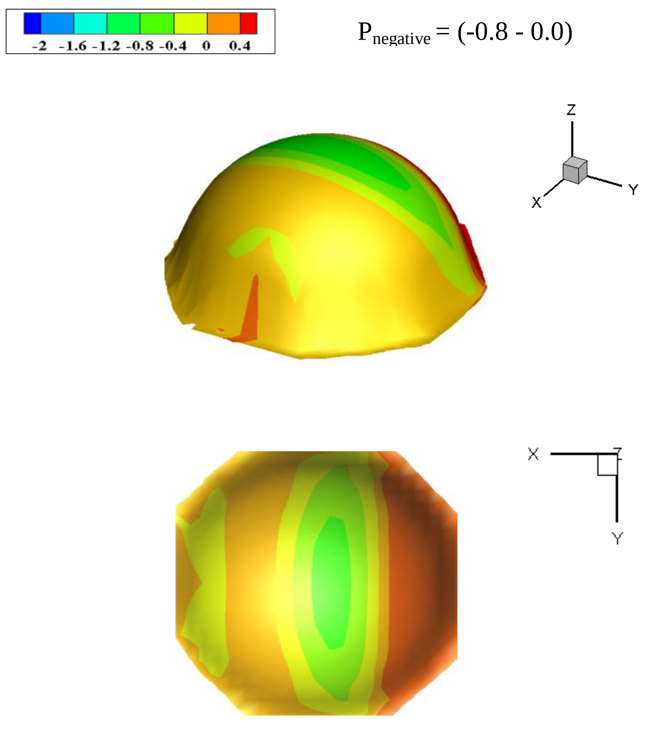

(a) The max. negative pressure coefficient contour plots for a dome

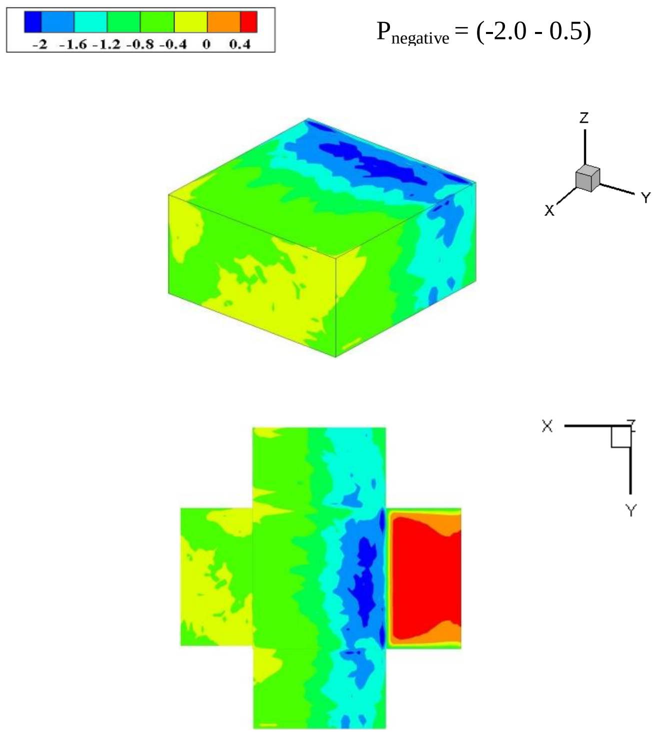

(b) The max. negative pressure coefficient contour plots for a prism

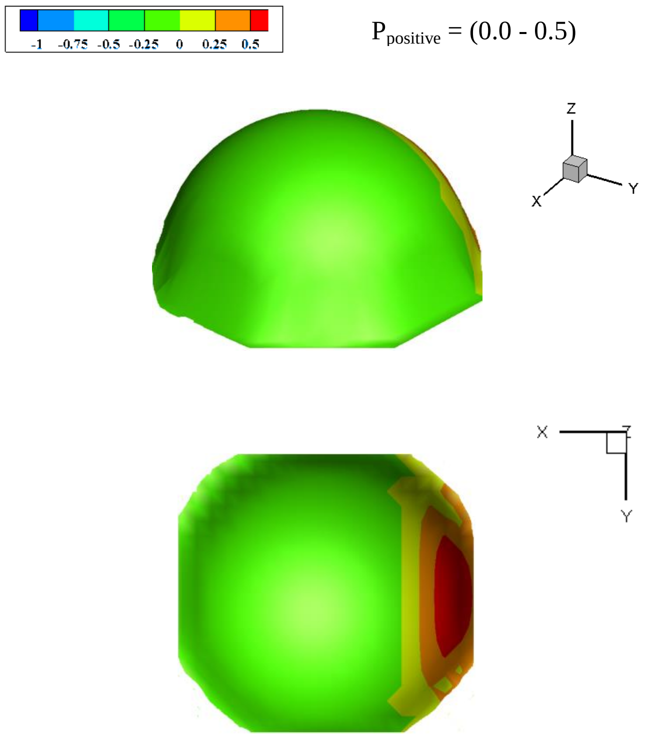

(c) The max. positive pressure coefficient contour plots for a dome

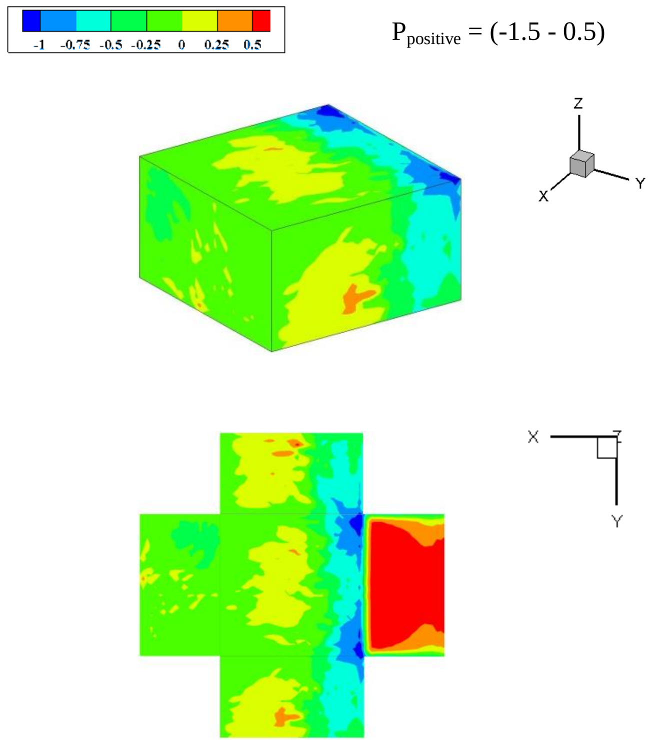

(d) The max. positive pressure coefficient contour plots for a prism

Figs. 9 The max. pressure coefficient contour plots due to effects of SL wind on dome and prism buildings

Table 2 Ratio between the maximum values of ASCE 7-10 and CFD simulation (ASCE 7-10/CFD) due to SL wind

Method	shape	Ax=Ay	Az	Cx	Cy	Cz	Cp
ASCE 7-10	dome	1.57	3.14	0.32	0.0	0.26	-0.8
CFD model	dome	1.57	3.14	0.32	0.0	0.25	-0.8
Maximum ratios of dome (ASCE/CFD)				1.00	----	1.04	1.0
ASCE 7-10	prism	1.77	3.14	0.85	0.0	0.84	-2.2
CFD model	prism	1.77	3.14	0.84	0.0	0.80	-2.0
Maximum ratios of dome (ASCE/CFD)				1.01	----	1.05	1.1

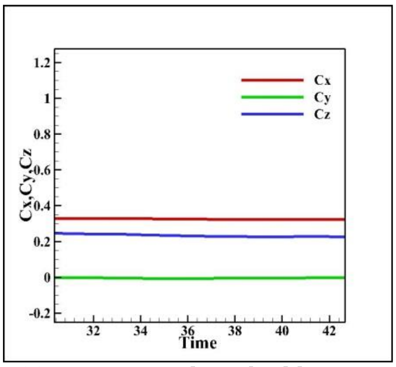

(a) Forces on a dome building

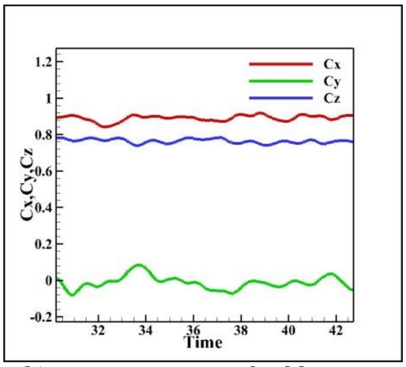

(b) Forces on a prism building

Fig. 10 The maximum force coefficients due to SL wind

For comparison, the prism model creates about 160 % higher overall force in the *x*-direction, and 220% higher overall suction force in the z-direction than the dome model.

The forces coefficients were calculated from ASCE 7-10 provisions for low-rise buildings. The Main Wind Force Resisting Systems (MWFRS) provisions were used for the force coefficients comparison. In addition, the Components and Cladding (C&C) provision were applied for the pressure coefficients comparison. The building is chosen to be in open terrain (Exposure *C*) and with homogenous topography. An importance factor of 1.0 (Category *2*) was considered for the present analysis with a design wind speed of 90 mph. Full-scale building dimensions were used for the force and moment calculation. Forces for the eight different building configurations given in the standard and worst case forces were normalized according to Eqs. (15)-(18) to compare with CFD model results.

The ratio between maximum values of the CFD model and the ASCE 7-10 are presented in Table 2. These data show that maximum force and pressure coefficients on dome and prism buildings from the ASCE 7-10 standard are close to those from the CFD model. However, the lateral force coefficient (in the x-direction) and pressure on dome induced by the SL winds using the CFD model is the same to those from ASCE 7-10 provisions.

3.2 Tornado-structure interaction and coefficients due to tornado wind

In this section, the tornado coefficients on dome and prism buildings are compared using CFD simulation.

3.2.1 Tornado vortex structure during the interaction with dome and prism

The primary advantage of CFD modeling of the tornado-structure interaction is the capability to investigate the wind characteristics for any building shape at any instant in time. The interaction of tornado wind with the dome and the prism at various instances of non-dimensional times (t = 10, 24, 35) are illustrated in Figs. 11(a)-11(f). At the time of 10 units, the vortex is in front of the building as shown in Figs. 11(a) and 11(b). At the time of 24 units, the low-level part of the vortex starts to interact with the building. As the vortex travels ahead, the vortex over the dome transports smoothly until it passes the building. However, the vortex over the prism starts to separate until it passes the building as illustrated in Figs. 11(c) and 11(d). Since the prism building has angles, sharp corners and flat surfaces, they give the wind something to lift or push against. Therefore, the vortex separates when it travels over the prism. However, the dome building does not have those features. The dome has smooth and rounded surfaces that make the vortex move smoothly over it. As the vortex moves away from the dome and the prism building at time t= 35, it starts to recover its initial cylindrical shape in Figs. 11(e) and 11(f).

3.2.2 Force and pressure coefficients due to tornado wind

The three-dimensional contours of the minimum and maximum tornado pressures for the dome and the prism buildings are illustrated in Figs. 12(a)-12(d). The absolute maximum negative and positive tornado pressures on the dome are - 2.0 and 1.0, respectively. The maximum effect of the negative pressure is seen close to the top of the dome and the positive pressure is seen closer to the ground. The absolute maximum negative and positive pressures on the prism are - 3.5 and 2.5 respectively. The maximum effect of the negative pressure is seen on the roof and walls of the prism close to the sharp edge and corners, and the positive pressure is seen more on the walls. The prism makes higher maximum negative and positive pressure than the dome model, about 75% and 150% more, respectively.

The tornado force coefficients for dome and prism models are calculated by integrating pressure all over the dome and prism buildings. The maximum *Cx, Cy,* and *Cz,* values for dome and prism buildings are 0.70,-0.70, 0.94; 1.40, -1.39, 2.60 (Figs. 13(a) and 13(b)). *Cx* and *Cz* are positive for the entire period of tornado-structure interaction and *Cy* moves from positive to negative. Here positive value means the force coefficients are acting in the direction of the positive axis. Consequently, *Cz* is an uplifting force on the roof. The side forces can pull or push depending upon the tornado position with respect to the structure. It is noticed that the prism makes higher tornado force coefficients than the dome, about 100 % more in the *x*- and *y*-directions and 180 % more in the *z*-direction. The domed shape created force and pressure coefficients less than cubic shape, either regular or rectangular because of the double curve. The double curve distributes pressure evenly throughout the structure, preventing stress from concentrating at one point.

3.3 Compare the force and pressure coefficients due to SL and tornado wind

The maximum force and pressure coefficients due to tornado and SL wind are compared. From the comparison, one can see that the tornado pressure coefficients from dome and prism are higher than SL wind by 150% and 75%, respectively (Figs. 9 and 12). The tornado forces coefficients on prism are also higher than those from SL wind. The force coefficients on prism due to the tornado wind are larger than those due to the SL wind, about 65% more in *x*-direction and about 225% more in *z*-direction. Selvam and Millett (2005) employed a large eddy simulation as turbulence model and obtained reasonable results for flow around a cube. They concluded the absolute maximum pressure induced by tornadic winds is found to be 40% more than that induced by SL winds. They concluded that the translating tornado produced about 100% force on the roof and about 45% more on the walls compared to wind loads. The results obtained from the current study are larger than those reported by Selvam and Millet (2005) because the grid refinement utilized in this work is far too coarse to adequately resolve flow around the structure. Haan *et al.* (2010) simulated loading of a typical cube and gabled residence. They report that lateral wall force coefficients and uplift produced on the roof are respectively 150% and 180% to 320% greater for tornado wind than for straight-line wind. Those results are in agreement with those that were reported in current study.

The side tornado forces coefficients on dome are higher than those from SL wind by 120%. The roof tornado coefficients on dome are higher than those from SL wind by 280% (Figs. 10 and 13). Zhao *et al.* (2016) studied the flow and pressure around a dome due to SL and tornado wind by moving the dome. They concluded absolute maximum pressure induced by tornadic winds is found to be 130% more than that induced by SL winds. The authors also reported that the wind vertical force coefficients obtained in the tornadic wind field is 270% more than those obtained in the SL wind field. The vertical force and pressure coefficients values are in agreements with those that were reported in the current study. However, the lateral force coefficient (in the x-direction) induced by the tornadic winds is 600% more than that induced by the SL winds. The lateral force coefficients (in the x-direction) obtained from the current study are smaller than those reported by Zhao *et al.* (2016) because they did not have proper grid resolution. In our comparison, the coefficients are calculated for the same maximum velocities and hence for the same maximum wind speed of the tornado wind.

4. Conclusions

A Large Eddy Simulation (LES) turbulence model and Rankine Combined Vortex (RCV) model were used to investigate tornado forces on dome and prism buildings. The conclusions arrived at from the completed work are listed below.

- The tornado force coefficients on the dome building are larger than forces due to SL wind, about 120% more in *x*- and *y*-direction and 280% more in *z*-direction. In addition, the tornado pressure coefficients are larger than pressure due to SL wind, about 150%.
- The force coefficients on prism due to the tornado wind are larger than those due to the SL wind, about 65% more in *x*-direction and about 225% more in *z*-direction. The tornado pressure coefficients are also greater, about 75%.
- The translating tornado wind produces higher overall force coefficients on the prism than dome, about 100% more in *x*- and *y*-directions and about 180% more in *z*-direction. In addition, the tornado pressure coefficients on prism are 150% greater.

Further work is underway by investigating different variables such as the height, projected area and volume for both the dome and prism building. Tornado parameters such as translational velocity, core size, and maximum tangential wind speed also will be investigated. With the more data collected, our findings are likely to provide new results of tornado effects on dome and prism type buildings.

Acknowledgements

The authors acknowledge and appreciate the computer support that is provided by the College of Engineering, University of Arkansas, for this work. The first author also acknowledges the financial support that is provided by Libyan Government scholarship.

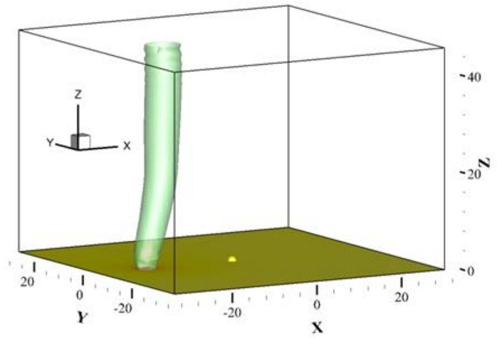

(a) The vortex-dome interaction at 10 units

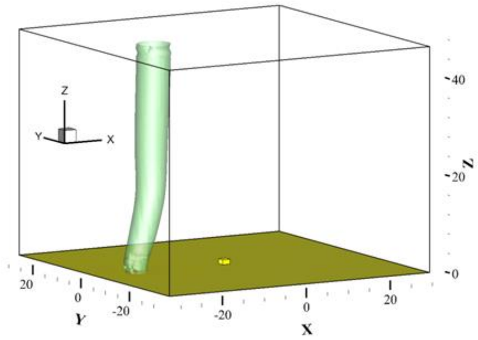

(b) The vortex-prism interaction 10 units

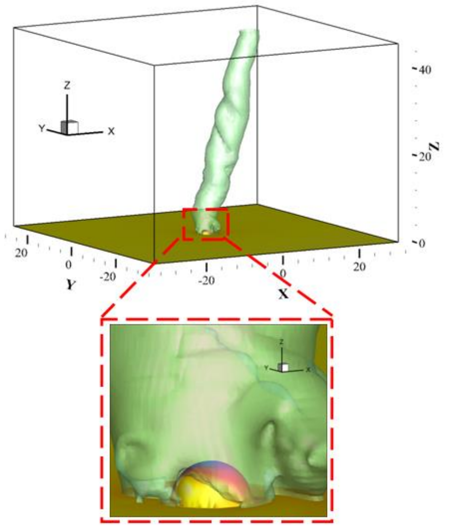

(c) The vortex-dome interaction at 24 units

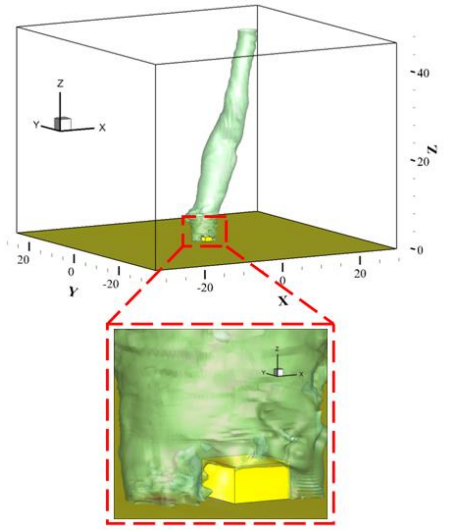

(d) The vortex-prism interaction 24 units

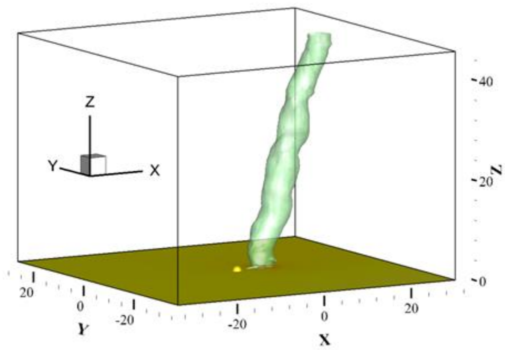

(e) The vortex-dome interaction at 35 units

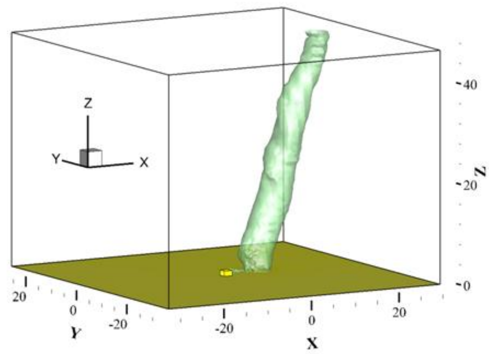

(f) The vortex-prism interaction 35 units

Fig. 11 Iso-pressure surfaces of the vortex-structure interaction

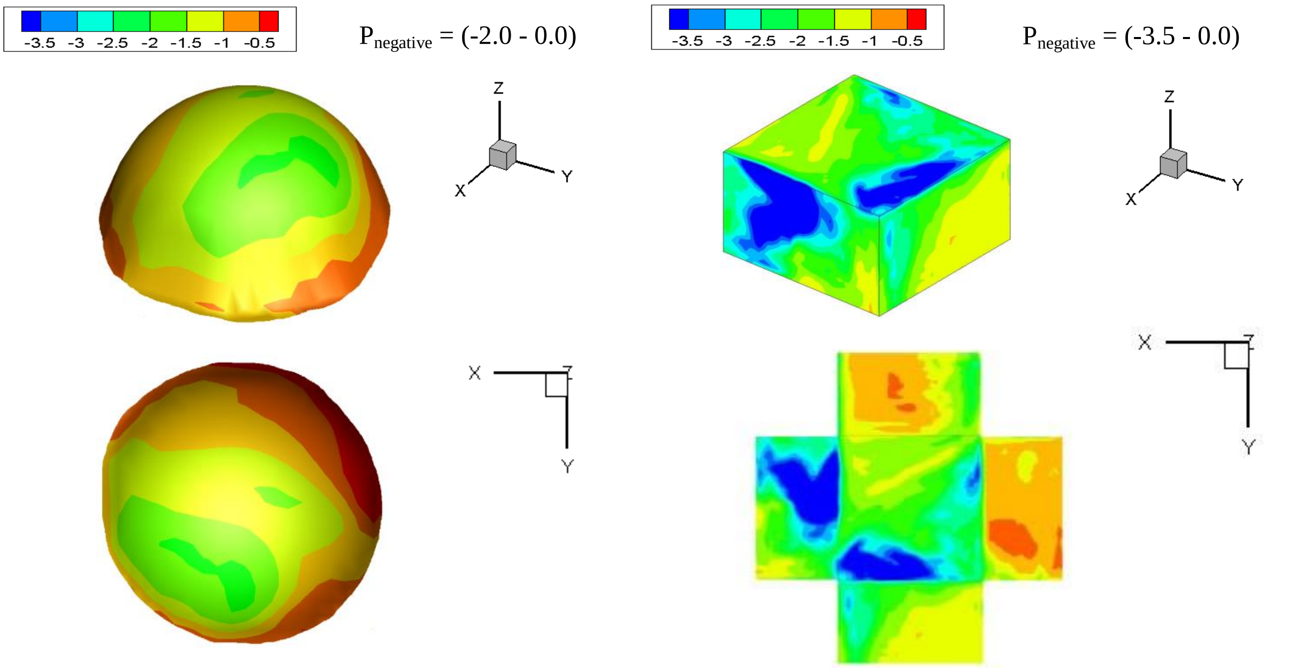

(a) The max. negative pressure coefficient contour plots for dome

(b) The max. negative pressure coefficient contour plots for prism

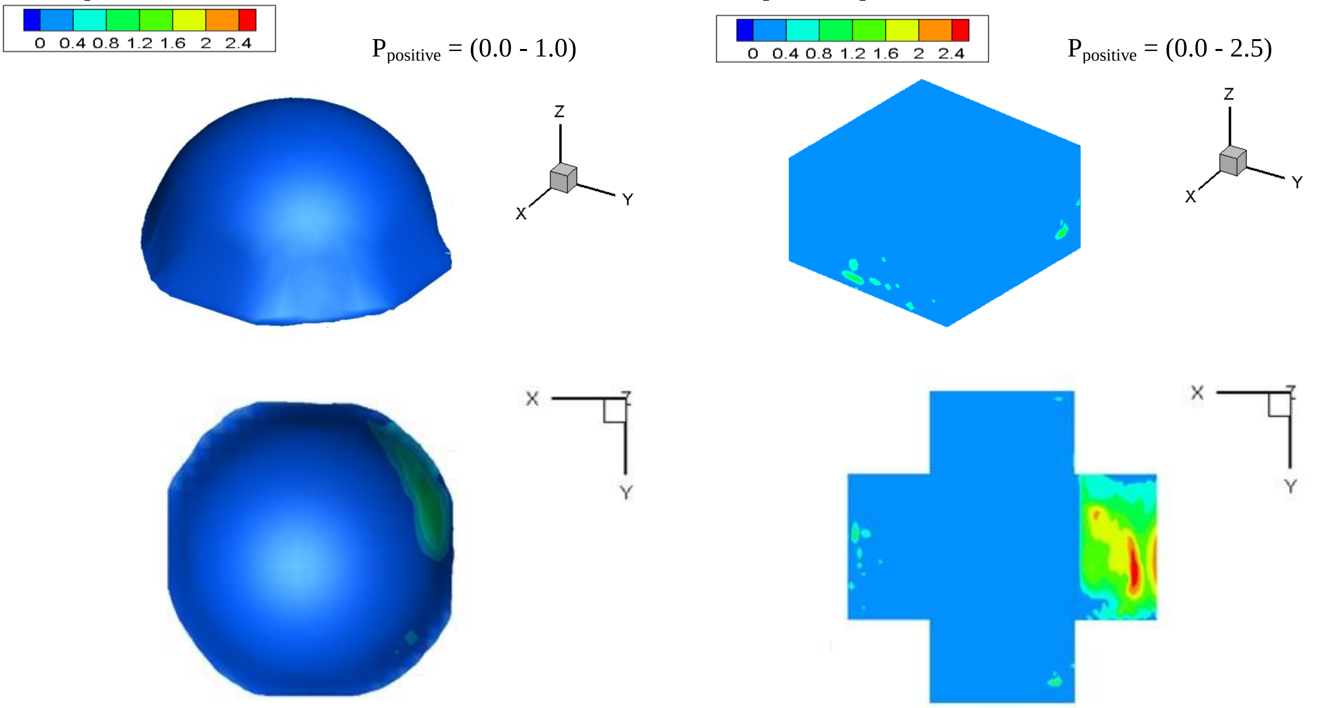

(c) The max. positive pressure coefficient contour plots for dome

(d) The max. positive pressure coefficient contour plots for prism

Fig. 12 The max. pressure coefficient contour plots due to effect of tornado wind on dome and prism buildings

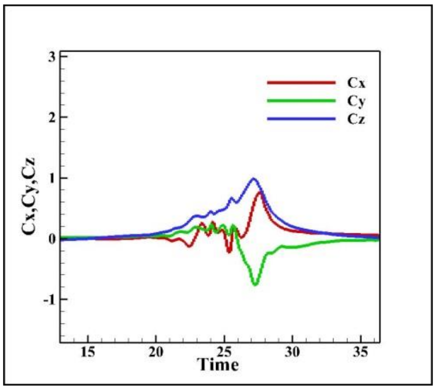

(a) Forces on dome building

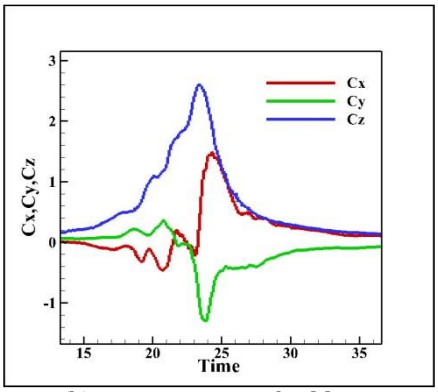

(b) Forces on prism building

Fig. 13 The maximum force coefficients due to tornado wind

References

Ahmed, S.N. and Selvam, R.P. (2015), "Ridge effects on tornado path deviation", *Int. J. Civil aStruct. Eng*., **3** (1), 273-294.

Alrasheedi, N.H. and Selvam, R.P. (2011), "Computing tornado forces on different building sizes", *Proceedings of the International Conference on Wind Engineering (ICWE13)*, Amsterdam, Netherlands.

Church, C., Burgess, D., Doswell, C. and Davies-Jones, R. (1993), "Tornado vortex theory, in: the tornado: its structure, dynamics, prediction, and hazards", *Geophys. Mono., American Geophys. Union.*, **79**, 19-39.

de Sampio, P.A.B, Lyra, P.R.M., Morgan, K. and Weatherill, N.P. (1993), "Petro-Galerkin solutions of the incompressible Navier-Stokes equations in primitive variables with adaptive remeshing", *Comput. Method. Appl. M.*, **106**, 143-178

Filippone, A. and Afgan, I. (2008), "Orthogonal blade-vortex interaction on a helicopter tail rotor", *AIAA J.*, **46** (6), 1476-1489.

Gorecki, M.P. and Selvam, R.P. (2015), "Rankine combined vortex interaction with a rectangular prism", *Int. J. Comput. Fluid. D.*, **29** (1), 120-132.

Gorecki, M.P. and Selvam, R.P. (2014), "Visualization of tornado-like vortex interacting with wide tornado-break wall", *J. Visualize.*, **18** (2), 393-406.

Haan, F.L., Balaramudu, V.K. and Sarkar, P.P. (2010), "Tornado-induced wind loads on a low-rise building", *J. Struct. Eng. - ASCE*, **136**(1), 106-116.

Hu, H., Yang, Z., Sarkar, P. and Haan, F. (2011), "Characterization of the wind loads and flow fields around a gable roof building model in tornado-like winds", *Exp. Fluids*, **51**(3), 835-851.

Ishihara, T., Oh, S. and Tokuyama, Y. (2011), "Numerical study on flow fields of tornado-like vortices using the LES turbulence model", *J. Wind Eng. Ind. Aerod*., **99**(4), 239-248.

Kosiba, K.A., Robinson, P., Chan, P.W. and Wurman, J. (2014), "Wind field of a non-mesocyclone anticyclonic tornado crossing the Hong Kong International Airport". *Adv. Meterorol.*, **2014**, 1-7.

Liu, X. and Marshall, J.S. (2004), "Blade penetration into a vortex core with and without axial core flow", *J. Fluid Mech*., **519**, 81-103.

Monolithic (2013), Testimonials/domers-respond-to-Moore-Oklahoma; Monolithic Dome Institute, Texas, USA, http://www.monolithic.org/testimonials/domers-respond-to-moore-oklahoma

Monolithic (2013), Monolithic dome school; Monolithic Dome Institute, Texas, USA, http://www.monolithic.org/schools

Murakami, S. and Mochida, A. (1995), "On turbulent vortex-shedding flow past 2D square cylinder predicted by CFD", *J. Wind Eng. Ind. Aerod.*, **54-55**, 191-211.

New Age Dome Construction (2017), Tornado Shelters/Domes in Disasters; New Age Dome Construction, Buncaville, USA, http://newagedomeconstruction.com/services/tornado-shelters/.

NWS (2011), National Weather Service Weather Forecast Office; Tuscaloosa-Birmingham Tornado, USA, http://www.srh.noaa.gov/bmx/?n=event_04272011tuscbirm.

NWS (2017), Tuscaloosa-Birmingham Tornado; National Weather Service, Birmingham, USA http://www.srh.noaa.gov/bmx/?n=event_04272011tuscbirm.

Rajasekharan, S.G., Matsui, M. and Tamura, Y. (2013), "Characteristics of internal pressures and net local roof wind forces on a building exposed to a tornado-like vortex", *J. Wind Eng. Ind. Aerod.*, **112**, 52-57.

Sabareesh, G.R., Matsui, M. and Tamura, Y., (2013), "Ground roughness effects on internal pressure characteristics for buildings exposed to tornado-like flow", *J. Wind Eng. Ind. Aerod.*, **122**, 113-117.

Strasser, M.N. and Selvam, R.P. (2015), "The variation in the maximum loading of a circular cylinder impacted by a 2D vortex with time of impact", *J. Fluid. Struct*., **58**, *66-78*.

Selvam, R.P. (1985), "Applications of the boundary element method for tornado forces on buildings", Ph.D. dissertation, Texas Tech University, Lubbock.

Selvam, R.P. (1993), "Computer modeling of tornado forces on buildings", *Proceedings of the 7th US National Conference on Wind Engineering*, Gary C. Hart, Los Angeles, June.

Selvam, R. P. (1997), "Finite element modelling of flow around a circular cylinder using LES", *J. Wind Eng Ind. Aerod*., **67-68**, 129-139.

Selvam, R.P. (1998), "Computational procedures in grid based computational bridge aerodynamics", *In Bridge Aerodynamics*, (Eds., *Larsen, A. and Esdahl*), Balkema, Rotterdam.

Selvam, R.P. and Gorecki, P. (2012), "Effect of tornado size on forces on thin 2D cylinder", *3rd American Association for Wind Engineering Workshop*, Hyannis, Massachusetts, USA.

Selvam, R.P. and Paterson, D.A., (1993), "Computation of Conductor Drag Coefficients", *J. Wind Eng Ind. Aerod*., **50**, 1-8.

Selvam, R.P. and Millett, P. (2003), "Computer modeling of tornado forces on buildings", *Wind Struct*., **6**(1), 209-220.

Selvam, R.P. and Millett, P. (2005), "Large eddy simulation of the tornado-structure interaction to determine structural loadings". *Wind Struct*., **8** (1), 49-60.

Selvam, R.P., Roy, U.K., Jung, Y. and Mehta, K.C. (2002), "Investigation of tornado forces on a 2D cylinder using computer modeling", *In Wind Engineering, by K. Kumar (Ed), Phoenix Publishing House,* New Delhi, India.

Sengupta, A., Haan, F.L., Sarkar, P.P. and Balaramudu, V. (2008), "Investigation of tornado transient loads on buildings in microburst and tornado wind", *J. Wind Eng Ind. Aerod*., **96**(10-11), 2173-2187.

Tamura, T. (1999), "Reliability on CFD estimation for wind-structure interaction problems", *J. Wind Eng. Ind. Aerod*., **81**(1), 117-143.

Tamura, T., Itoh, Y., Wada, A. and Kuwahara, K. (1995), "Numerical study of pressure fluctuations on a rectangular cylinder in aerodynamic oscillation", *J. Wind Eng Ind. Aerod*., 54, 239-250.

Wen, Y. (1975), "Dynamic tornadic wind loads on tall buildings", *J. Struct. Div*., **101** (1), 169-185.

Wurman, J., Kosiba, K. and Robinson, P. (2013), "In situ, Doppler radar, and video observations of the interior structure of a tornado and the wind-damage relationship", *Bull. Am. Meteorol. Soc*., **94**(6), 835-846.

Wurman, J., Robinson, P., Alexander, C. and Richardson, Y. (2007), "Low-Level Winds In Tornadoes And Potential Catastrophic Tornado Impacts In Urban Areas", *Bull. Am. Meteorol. Soc*., **88**(1), 31-46.

Yang, Z., Sarkar P.P. and Hu, H. (2010), "Visualization of flow structures around gable-roofed building model in tornado-like winds", *J. Visualize.*, **13,** 285-288.

Yousef, M.A. and Selvam, R.P. (2016), "Effect of equivalent height, surface area and Volume of the dome to prism on tornado forces using CFD", *Proceedings of the 8th International Colloquium on Bluff Body Aerodynamics and Applications (BBAA VIII),* Boston, Massachusetts, June.

Zhao, Y., Yan, G., Zu, J., Yuan, F., Kakkattukuzhy, M. and Isaac, K. (2016), "Comparison on wind effects of tornadic and straight-line wind fields on spherical dome structures", *Proceedings of the 8th International Colloquium on Bluff Body Aerodynamics and Applications (BBAA VI*II)", Boston, Massachusetts, June.

AD